Competition between a Lamellar and a Microemulsion Phase in an Ionic Surfactant System

Willem K. Kegel and Henk N. W. Lekkerkerker*

Van't Hoff Laboratory, University of Utrecht, Padualaan 8, 3584 CH Utrecht, The Netherlands

Received: June 1, 1993; In Final Form: August 2, 1993®

An experimental study of a microemulsion system consisting of equal volumes of brine (water plus salt) and oil (cyclohexane), sodium dodecyl sulfate (SDS) as surfactant, and a mixture of hexanol and pentanol as cosurfactant is presented. Increasing the hexanol fraction in the cosurfactant mixture causes a competition between the (disordered) microemulsion phase and a lamellar phase at vanishing spontaneous curvature, culminating in four-phase brine–lamellar phase–microemulsion phase–oil coexistence. A SAXS study of the lamellar phases is presented. Although a rather high salt concentration was used (0.2 M NaCl), several indications for the presence of electrostatic repulsion between the lamellae are found. When the dispersion size ξ of the middle-phase microemulsion exceeds the value of approximately 70 nm, the lamellar phase becomes stable in the presence of excess oil and water. A similar dispersion size is estimated for a nonionic surfactant system where the lamellar phase is close to the three-phase body (Kahlweit, M.; Strey, R.; Firman, P. *J. Phys. Chem.* **1986**, *90*, 671). The experimentally observed phase behavior is compared with a phenomenological theory (Andelman, D.; Cates, M. E.; Roux, D.; Safran, S. A. *J. Chem. Phys.* **1987**, *87*, 7229). It appears that the theory qualitatively correctly describes the competition between the microemulsion and the lamellar phases. However, quantitatively there is a difference between theory and experiment which is attributed to the effect of a negative Gaussian bending elastic modulus.

Introduction

Microemulsions are dispersions of water and oil into one another stabilized by one or more surfactants. They differ markedly from molecular solutions as oil and water are found in domains of order 1–10 nm in size. This results in an extensive oil–water interface covered with a monolayer of adsorbed surfactant molecules. Commonly observed structures of the oil and water domains range from water droplets in oil or *vice versa* at asymmetric water/oil ratios to bicontinuous and liquid crystalline at comparable volume fractions. The latter are usually found at relatively high amounts of surfactant (more than a few weight percent). In the past few years, much work has been done on the phase behavior of microemulsion systems, experimental (for reviews, see refs 1 and 2) as well as theoretical.[3-8] An impressionistic representation of the phase diagram corresponding to equal volumes of water and oil is presented in Figure 1.

Figure 1 shows the characteristic "fish" shape. The cosurfactant or salt concentration (in case of ionic surfactants) tunes the curvature of the surfactant monolayer. At low surfactant concentrations and increasing cosurfactant/salt concentration, the (continuous) phase transitions Winsor I (oil droplets in water in equilibrium with excess oil)–Winsor III (present in the "body" of the fish, a middle-phase microemulsion coexisting with both water and oil)–Winsor II (water droplets in oil in equilibrium with excess water) are observed. Increasing the surfactant concentration starting in the body of the fish leads to an increase of the middle-phase volume at the expense of the oil and water phases and eventually gives rise to a monophasic microemulsion system. Upon further increase of the surfactant concentration, a first-order transition to a lamellar phase may occur. In three-component systems consisting of oil, water, and a nonionic surfactant (usually referred to as "nonionics"), the role of salt and/or cosurfactant is replaced by the temperature.[1]

One of the thermodynamic models of microemulsion phase behavior is based on the "phenomenological" approach[5,6] which was initiated by Talmon and Prager[3] and further developed by de Gennes and co-workers.[4] In this approach, the surfactant monolayer is considered as an incompressible two-dimensional fluid separating oil and water regions. The phase behavior of the system is determined by the curvature energy of the monolayers and the entropy of mixing of the oil and water domains. At an oil/water ratio of about 1 and without any tendency of the surfactant monolayer to curve either toward water or toward oil (i.e., zero spontaneous curvature), these models predict a competition between a microemulsion (bicontinuous) phase and a lamellar liquid crystalline phase.

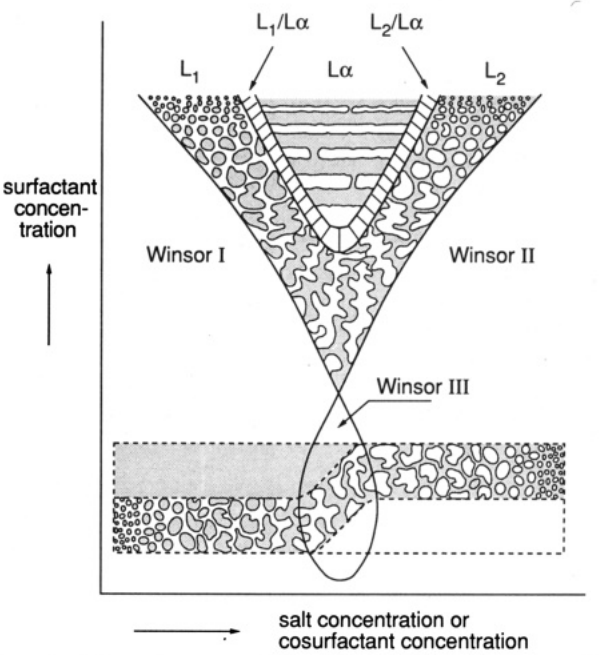

Figure 1. Schematic representation of a typical phase diagram of a microemulsion system at an oil/water ratio equal to 1, modeled after Strey[9] and van Aken.[10]

In this paper, we report an experimental study concerning this microemulsion–lamellar phase competition in a system composed of brine (water plus salt), cyclohexane, sodium dodecyl sulfate (SDS) as surfactant, and pentanol/hexanol cosurfactant mixtures. Upon increasing the hexanol fraction in the system, the lamellar

* Author to whom correspondence should be addressed.
® Abstract published in *Advance ACS Abstracts*, September 15, 1993.

0022-3654/93/2097-11124$04.00/0

phase becomes stable at increasingly lower surfactant concentration. This trend eventually leads to a penetration of the lamellar phase into the three-phase body, giving rise to an intricate phase behavior including a four-phase equilibrium brine, lamellar phase, microemulsion phase, oil.[11,12] The dispersion size ξ and the interlamellar distance D in the microemulsion and lamellar phases obtained from the compositions and from SAXS measurements are discussed. Interestingly, the length scale ξ in the microemulsion phase in the four-phase equilibrium is close to the one in a nonionic system where the lamellar phase closely approaches the three-phase body.[13] In the next section, we will summarize some aspects of the phenomenological model that are relevant for the interpretation of the work presented here.

Theory

The characteristic features of the phase behavior schematically depicted in Figure 1 have been successfully explained by a simple phenomenological interfacial model.[5,14] In this model, the microemulsion phase is described with the help of a cubic lattice of side ξ. The probability of an elemental cell of the lattice containing water and oil is ϕ and $(1 - \phi)$ with ϕ related to the volume fractions of water (ϕ_w), oil (ϕ_o), and surfactant (ϕ_s): $\phi = \phi_w + \phi_s/2$ and $(1 - \phi) = \phi_o + \phi_s/2$. The incompressible surfactant monolayer of thickness a is constrained to reside between the oil and water domains. Using a random mixing approximation (i.e., the probability of a cell side to be covered with a surfactant layer is just $\phi(1 - \phi)$), the lattice size ξ is determined by the composition of the microemulsion phase

$$\xi/a = 6\phi(1 - \phi)/\phi_s \tag{1}$$

Interestingly, in a variety of microemulsion systems Langevin and co-workers[15] found a convincing agreement between ξ as determined from eq 1 and the length scale π/q_{max} obtained from a correlation peak at $q = q_{max}$ determined by SAXS and SANS.[15] The free energy density of the microemulsion phase, $F_{\mu E}$, can be written as the sum of the entropy of mixing per unit volume, S, and the curvature energy density, F_c

$$F_{\mu E} = F_c - TS \tag{2}$$

with

$$S = -k_B(\phi \ln \phi + (1 - \phi) \ln(1 - \phi))/\xi^3 \tag{3}$$

and F_c in the case of vanishing spontaneous curvature

$$F_c = 8\pi\phi(1 - \phi)K(\xi)/\xi^3 \tag{4}$$

The last equation is based on the association of a bend in the cubic lattice with a section of a sphere of diameter ξ. $K(\xi)$ is the renormalized bending elastic modulus. The renormalization takes into account the thermal fluctuations of the surfactant monolayer at length scales smaller than ξ

$$K(\xi) = K_0 - \frac{\alpha k_B T}{4\pi} \ln(\xi/a) \tag{5}$$

with α a constant for which values of 1[16] and 3[17] have been predicted and K_0 the bending elastic modulus at the molecular length scale a. At constant ϕ, it follows from eqs 1–5 that the free energy of the microemulsion phase is essentially of the form

$$F_{\mu E} = [A + B \ln \phi_s]\phi_s^3 \tag{6}$$

with (at equal volumes of brine and oil i.e., $\phi = 1/2$)

$$A = \frac{8}{27a^3}\left(2\pi K_0 + k_B T\left[\ln(1/2) - \frac{\alpha}{2}\ln(3/2)\right]\right)$$

$$B = \frac{4\alpha k_B T}{27a^3}$$

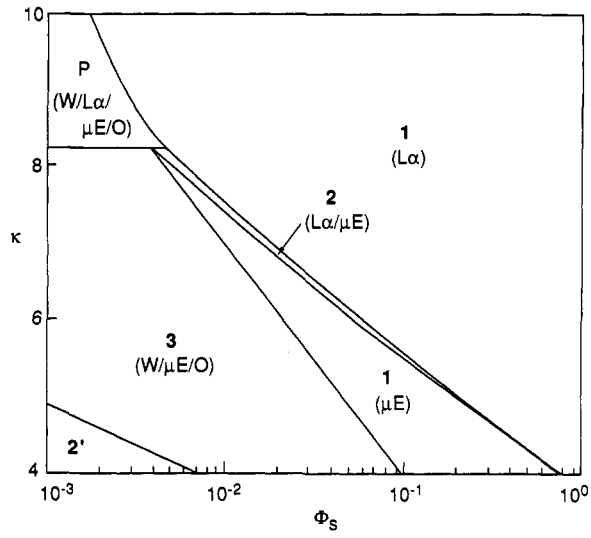

Figure 2. Phase boundaries in the $\kappa = 4\pi K_0/k_B T - \phi_s$ plane at equal volumes of brine and oil and vanishing spontaneous curvature from Cates et al.[14] The regions denoted 2, 3, and 1 correspond to almost pure water and oil, Winsor III equilibrium, and a single-phase microemulsion. 2 and "P" are a two-phase lamellar–microemulsion coexistence region and a region corresponding to "complex polyphasic equilibria between water, oil, lamellar phase and microemulsion phases with a water/oil ratio different from 1".

The free energy density of the lamellar phase, $F_{L\alpha}$, is estimated by generalizing Helfrich's result[18] concerning the confinement free energy of a symmetric fluctuating membrane in a stack of other membranes. The result is

$$F_{L\alpha} = c\frac{(k_B T)^2}{K_0 a^3}[\phi^{-2} + (1 - \phi)^{-2}]\phi_s^3 \tag{7}$$

with c of order 1/100.[18] At constant ϕ, the free energy of the lamellar phase essentially scales as ϕ_s^3. The phase diagram is calculated by double tangent constructions on eqs 6 and 7 (the three-phase coexistence was found by first minimizing eq 6 with respect to ϕ and then with respect to ϕ_s). The result in the $\kappa = 4\pi K_0/k_B T - \phi_s$ plane is shown in Figure 2 (taken from Cates et al.[14]) where $\alpha = 1$ and $c = 0.15/4\pi$ was used.

From eqs 6 and 7, it follows that in this model the phase transition microemulsion–lamellar is determined by the value of K_0. The link between theory and experiment in the case of nonionic surfactant systems is established by assuming that K_0 increases with increasing surfactant chain length. As a consequence of the logarithmic renormalization of the bending elastic modulus K (eq 5), the phase boundaries are nearly linear in the semilogarithmic representation of Figure 2. In fact, the theory predicts a strictly linear relation between the logarithm of the dispersion size ξ in the microemulsion phase and the bending elastic modulus K_0, which is reflected in the straight boundary between the Winsor III equilibrium and the one-phase microemulsion in the representation of Figure 2. This has been verified by Langevin,[15] who showed that for various surfactant systems ln ξ indeed seems to be linearly proportional to K_0. The above analysis only involves the bending elastic modulus K but neglects the Gaussian bending elastic modulus $\bar{K}$. This quantity is of importance in phase transitions where the genus of the surface is changed, which is indeed the case in the microemulsion–lamellar transition. The free energy contribution F_g associated with the Gaussian bending elastic modulus has been estimated within the random mixing model for $\phi = 1/2$ as[19]

$$F_g = -\pi\bar{K}/\xi^3 \tag{8}$$

Including this contribution to the free energy density of the microemulsion phase $F_{\mu E} = F_c + F_g - TS$ leaves the form of eq 6 unchanged but the coefficient A is now given by the expression

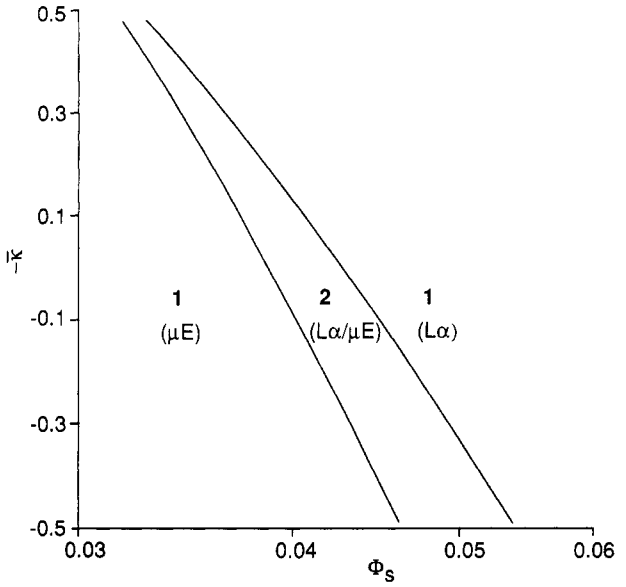

Figure 3. Phase boundaries in the $\bar{\kappa} = 4\pi\bar{K}/k_BT - \phi_s$ plane at constant $\kappa = 4\pi K_0/k_BT = 6.28$, equal volumex of brine and oil and vanishing spontaneous curvature.

$$A = \frac{8}{27a^3}\left(\pi(2K_0 - \bar{K}) + k_BT\left[\ln(1/2) - \frac{\alpha}{2}\ln(3/2)\right]\right) \quad (9)$$

from which it follows that both a positive K_0 and a negative $\bar{K}$ destabilize the microemulsion phase. Using the above expression for A, the influence of $\bar{K}$ on the phase boundaries between the microemulsion and the lamellar phase can now be calculated by double tangent constructions on eqs 6 and 7. The results are presented in Figure 3.

From Figures 2 and 3, it is clear that both a decreasing $\bar{K}$ and an increasing K_0 may cause the phase transition microemulsion–lamellar.

Experimental Section

Materials. Sodium dodecyl sulfate (SDS) was a "specially pure" grade purchased from BDH. Cyclohexane, 1-pentanol, 1-hexanol, and NaCl (Baker) were "analyzed" grade. All chemicals were used without further purification. Deionized water was doubly distilled before use.

Preparation of the Samples. Eight grams (and in a number of cases 4.00 g) of initial oil phase was carefully poured on 10.00 g (or 5.00 g) of initial water phase in glass tubes with Teflon-sealed screw caps. The initial oil phase consisted of cyclohexane and various amounts of 1-pentanol plus 1-hexanol. The water phase was composed of 0.20 M NaCl and various concentrations of SDS. Equilibrium was attained by gently rolling the samples on a roller bench (ca. 1 rev/min) for several days. Subsequently, the samples were permitted to equilibrate at constant temperature (25 ± 0.1 °C) until no change in phase volumes was observed. Depending on the alcohol mixture used, the time necessary to obtain complete phase separation varied from less than 1 week (pure pentanol) to several months (pure hexanol).

In the single-phase lamellar systems in which the interlamellar spacing as a function of the SDS concentration was measured, repartition of cosurfactant between water, oil, and monolayers was prevented by the addition of two alcohol molecules with every SDS molecule.[22]

Polarization Microscopy. Birefringent phases were characterized using polarization microscopy. The observations were made with a Leitz Metallux 3 optical microscope equiped with a Linkman THMS 600 hot stage element. The qualification "lamellar phase" is reserved for birefringent phases showing a focal conics texture.[20]

Determination of Sample Compositions. The volume fraction of oil ϕ_0 (cyclohexane plus pentanol or hexanol) was determined by a Packard Model 433 gas chromatograph equipped with a flame ionization detector and a glass column packed with cross-linked polystyrene resin. The weight fraction of SDS, x_s, was obtained by evaporating the liquid components of a (weighted) sample. Correction for the amount of NaCl was carried out. From ϕ_0, x_s, and the density of SDS (1.45 g cm^{-3}), the volume fraction of water, ϕ_w, was calculated.

Small-Angle X-ray Scattering. SAXS measurements were made with an "Anton Paar" Kratky camera. The radiation source was a Philips broad-focus Cu X-ray tube (type PW2253/11) emitting Cu Kα radiation (wavelength 0.1542 nm). The scattered intensity is determined by two NaI scintillation counters (type ST-61-I/B) coupled to photomultipliers (EG&G Ortec Model 276) equipped with (EG&G Ortec) amplifiers. One detector is attached to the rear of the vacuum chamber and measures the scattering curve at a distance of 170 mm from the sample. The other detector is mounted above the collimation block and simultaneously monitors the stray radiation occurring there. By dividing the SAXS intensities through the corresponding signals of the monitor counter, they are normalized for the measuring time and corrected for fluctuations in the beam intensity. A constant temperature of 25.0 °C in the sample holder was maintained using a (Julabo) thermostatic bath coupled to a Pt-100 resistor element. Samples were measured in Mark-Röhrchen capillaries with a path length of 2 mm.

Results

Phase Behavior. The phase diagrams at different pentanol/hexanol ratios in the cosurfactant mixture are given in Figure 4a–e. Equal volumes of water phase (0.2 M NaCl plus SDS) and oil phase (cyclohexane plus cosurfactant mixture) were used. SDS concentrations are given in weight fractions in the total system, and alcohol mixture concentrations are given in weight fractions in the initial oil phase. Figure 4a–e corresponds to hexanol fractions x_h in the cosurfactant mixture pentanol plus hexanol of $x_h = 0.00, 0.25, 0.50, 0.75$, and 1.00, respectively, with $x_h = m_h/(m_p + m_h)$ in which m_h and m_p denote the mass of hexanol and pentanol.

For $x_h = 0$, 0.25, 0.50, and 0.75, the well-known progression of phase equilibria—Winsor I, Winsor III, Winsor II—is observed with increasing cosurfactant concentration at low SDS concentration (which depends on x_h: $x_s < 0.023$ for $x_h = 0$, $x_s < 0.018$ for $x_h = 0.25$, $x_s < 0.014$ for $x_h = 0.50$, and $x_s < 0.012$ or $x_h = 0.75$). Increasing the SDS concentration starting from the Winsor III region along the path A–B as indicated in Figure 4a (corresponding to a "balanced microemulsion" i.e., $c_0 = 0$) leads to a single-phase microemulsion system at increasingly lower surfactant concentration upon increasing x_h. At still higher surfactant concentrations, a first-order phase transition to a lamellar phase takes place (the dashed regions indicated in Figure 4a–d). Finally, the system is monophasic lamellar. On decreasing or increasing the cosurfactant concentration in the lamellar system, first-order phase transitions to the L_1 phase (oil droplets in water) and the L_2 phase (water droplets in oil) are observed, respectively. Going from $x_h = 0.00$ to $x_h = 0.75$, we observe that at low SDS concentrations the amount of cosurfactant in the system necessary to reach the middle-phase region (i.e., the region between Winsor I and Winsor II phase equilibria) is lowered, and the concentration range over which it is stable becomes significantly smaller. Moreover, the surfactant concentration at which the middle phase swells up to a one-phase microemulsion system decreases, and the lamellar phase becomes stable at increasingly lower surfactant concentrations in such a way as to approach the body of the fish. Using pure hexanol (Figure 4e), this trend is extended, resulting in a rather different pattern of phase behavior. At low SDS concentrations (less than about 0.011 w/w) and increasing hexanol

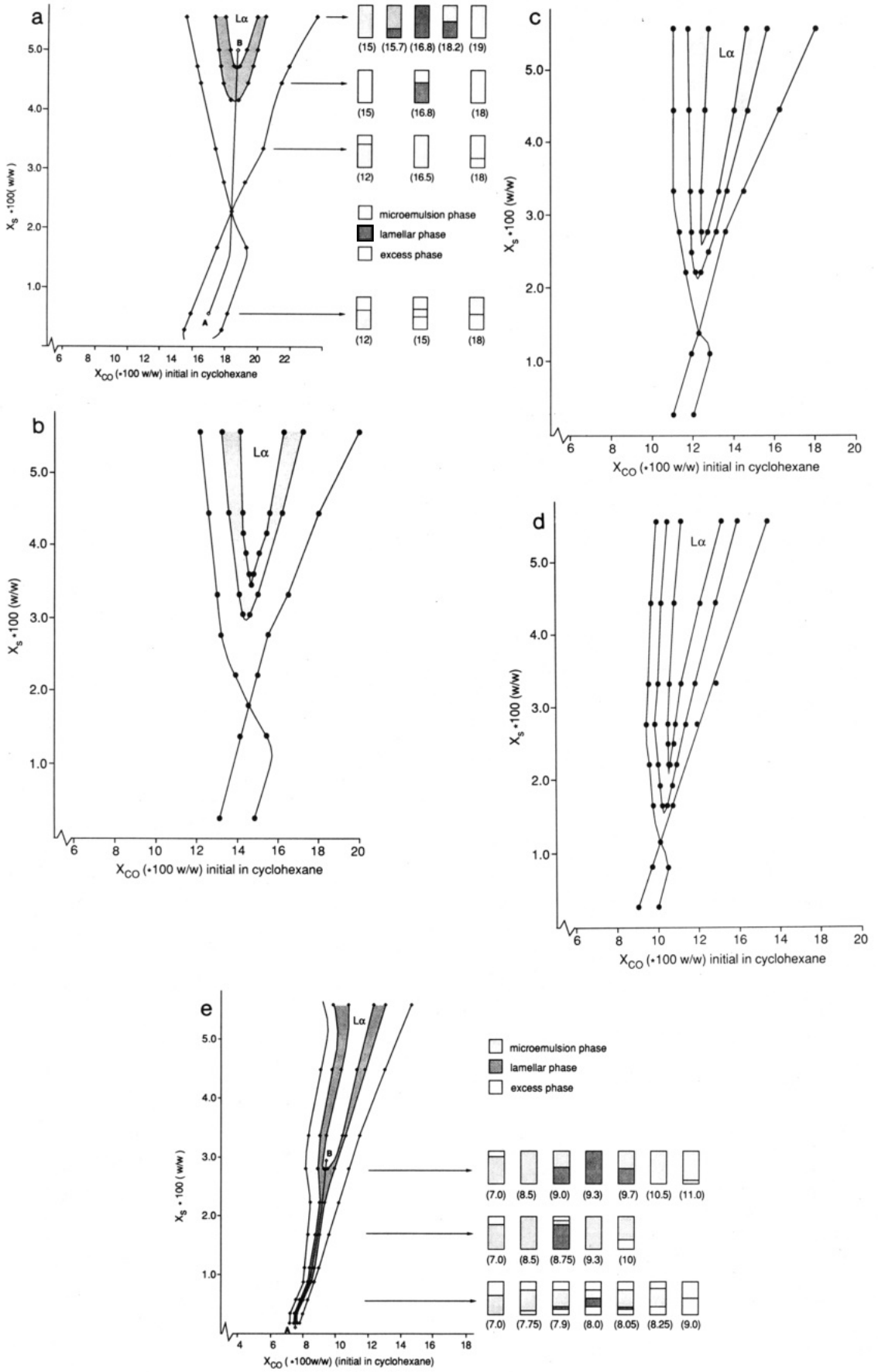

Figure 4. Phase behavior of brine (0.2 M NaCl), cyclohexane, SDS, and cosurfactant in the SDS–cosurfactant concentration (i.e., the initial weight fraction of the cosurfactant mixture in the oil phase) plane with equal volumes of brine and oil phases as a function of the hexanol weight fraction x_h in the cosurfactant mixture pentanol plus hexanol: $x_h = 0.00$ (pure pentanol, a), $x_h = 0.25$ (b), $x_h = 0.50$ (c), $x_h = 0.75$ (d), and $x_h = 1.00$ (pure hexanol, e). Shaded regions in the phase diagrams correspond to a lamellar phase in equilibrium with one or more isotropic phases. The pictograms are on-scale representations of the relative volumes of the coexisting phases. The cosurfactant concentrations are indicated between brackets.

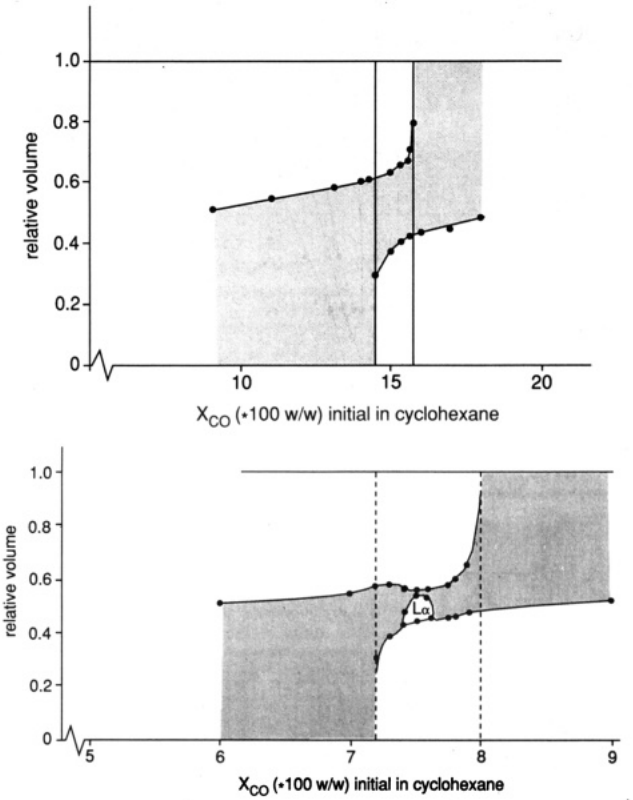

Figure 5. Relative volumes of the surfactant-rich phase(s) (indicated as shaded regions) as a function of the cosurfactant concentration in a system with $x_h = 0.00$ (pure pentanol) with an initial SDS weight fraction of 0.006 (a, top) and a system with $x_h = 1.00$ (pure hexanol) with an initial SDS weight fraction of 0.0014 (b, bottom).

concentration, the following sequence of phase equilibria is observed: Winsor I, Winsor III, four-phase equilibrium (water, lamellar phase, microemulsion phase, oil), Winsor III, Winsor II. In the four-phase equilibrium region, the volume of the lamellar phase first increases, reaches a maximum, and then decreases upon increasing the cosurfactant concentration, while the total volume of the surfactant rich phases remains approximately constant. Although it took several months to obtain a four-phase equilibrium, the system showed birefringence immediately after the addition of the components (for this purpose a 2-mm cuvette was used because of the high turbidity of the system). This is a clear indication that the lamellar phase is not a "pseudo lamellar phase" induced by gravity which has been observed in nonionic systems with a large dispersion size in the middle-phase region.[21]

In Figure 5, the relative volumes of the microemulsion phase and the lamellar phase as a function of the cosurfactant concentration at low SDS concentrations are given for $x_h = 0.00$ (Figure 5a, only a microemulsion middle phase present) and $x_h = 1.00$ (Figure 5b). The figure illustrates that in the pentanol system the phase volumes vary continuously going from Winsor I to Winsor II upon increasing the cosurfactant concentration. For the hexanol system, there seem to be small jumps at the hexanol concentrations at which the lamellar phase appears. These "jumps" in total surfactant-rich phase volume are small, indicating that the length scales in the microemulsion and in the lamellar phase are comparable. Looking at Figure 5b, it follows that between hexanol concentrations 7.50 and 7.56 % w/w the volume of the microemulsion phase is reduced to about 10% of the total surfactant-rich phase. This suggests that a small range of hexanol concentrations could exist for which a triphasic brine–lamellar–oil equilibrium occurs. In view of the large number of samples closely spaced in surfactant and cosurfactant concentration we have studied, we think this is rather unlikely unless this triphasic

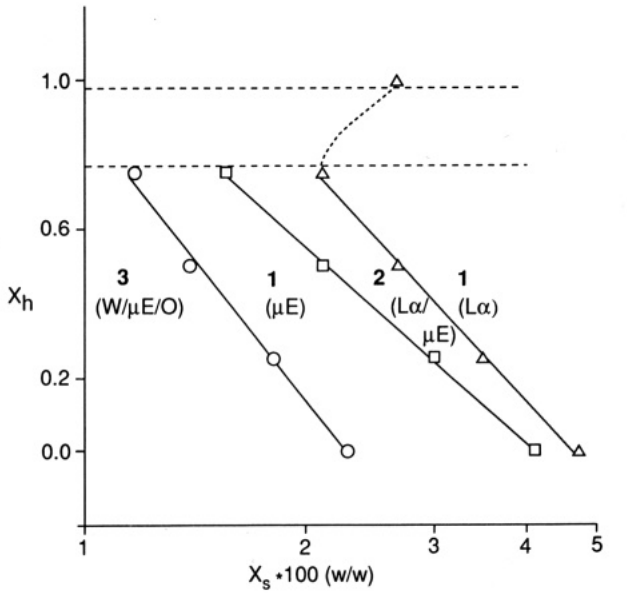

Figure 6. Phase boundaries at $c_0 \simeq 0$. Symbols ○, □, and △ represent boundaries between Winsor III/one-phase microemulsion, one-phase microemulsion/microemulsion–lamellar phase coexistence, and microemulsion–lamellar phase/single lamellar phase, respectively. Between the boundaries indicated by the dashed lines, a four-phase equilibrium appears.

system is stable over a very narrow cosurfactant concentration range of about 0.01% (w/w).

Increasing the SDS concentration in the hexanol system starting from the middle of the middle-phase region along the path A–B as indicated in Figure 43, the volumes of the surfactant-rich phases increase at the expense of the excess phases. However, while the middle-phase volumes increase linearly with the amount of SDS in the systems with $x_h \leq 0.75$, this is not the case in the hexanol systems for SDS concentrations above about 0.006 w/w. This is reflected in the compositions of the coexisting phases, which is discussed in the next section. The lamellar phase preferentially takes up water, resulting in a three-phase equilibrium (lamellar–microemulsion–excess oil) somewhat above 0.011 w/w SDS. At about 0.020 w/w SDS, a two-phase equilibrium (lamellar–microemulsion) and a single lamellar phase exist above 0.027 w/w SDS. Interestingly, this latter value is significantly higher than the minimum surfactant concentration of 0.021 w/w required for the formation of a single lamellar phase in the system with $x_h = 0.75$.

In Figure 6, the phase boundaries at $c_0 \simeq 0$ between Winsor III–one-phase microemulsion (further referred to as the 3–1 line)–two-phase microemulsion/lamellar (the 1–2 line) and one-phase lamellar systems (the 2–1 line) as a function of the weight fraction of SDS for systems with different hexanol mass fractions are shown. Looking at Figure 6, it follows that up to a hexanol mass fraction of $x_h = 0.75$ the boundaries between the phases are almost linear in this semilogarithmic representation, but the extrapolated 3–1 and 1–2 lines do not intersect at $x_h \leq 1$, as they should. We will come back to this point in the Discussion section.

Compositions of the Coexisting Phases. In Table I, the compositions of the equilibrated phases in the pentanol ($x_p = 0.00$) and hexanol ($x_h = 1.00$) systems at several SDS concentrations along the path A–B corresponding to a "balanced system", as indicated in parts a and e of Figure 4, are given.

In the case of pentanol, the SDS concentrations in the coexisting lamellar and microemulsion phases (between SDS concentrations of 0.043 and 0.047 w/w correspond to the values at the boundaries of the coexisting region, as they should in a first-order phase transition. From gas chromatography measurements, it was found that the pentanol concentration in the lamellar phases is somewhat higher than the pentanol concentration in the microemulsion

TABLE I: Composition of the Phases with Pure Pentanol and Hexanol as a Cosurfactant[a]

total SDS concn (g/g)	coexisting phases	composition phases			
		phase	x_s	ϕ_o	ϕ_w
		Pentanol System			
0.0431	$L_\alpha/\mu E$	$L\alpha$	0.047	0.468	0.509
		μE	0.041	0.500	0.480
0.0472	$L_\alpha/\mu E$	L_α	0.047	0.485	0.492
		μE	0.041	0.510	0.470
		Hexanol System			
0.0028	$B/L_\alpha/\mu E/O$	$L\alpha$	0.015	0.369	0.621
		μE	0.012	0.564	0.425
0.0056	$B/L_\alpha/\mu E/O$	L_α	0.015	0.341	0.647
		μE	0.012	0.560	0.429
0.0083	$B/L_\alpha/\mu E/O$	$L\alpha$	0.019	0.312	0.681
		μE	–	–	–
0.0111	$B/L_\alpha/\mu E/O$	$L\alpha$	0.022	0.320	0.669
		μE	0.020	0.524	0.465
0.0167	$L_\alpha/\mu E/O$	$L\alpha$	0.025	0.334	0.653
		μE	0.022	0.546	0.443
0.0250	$L_\alpha/\mu E$	$L\alpha$	0.027	0.485	0.512
		μE	0.025	0.522	0.461

[a] x_s is the determined weight fraction in the coexisting phases, and B, L_α, μE, and O denote excess aquous phase, lamellar phase, microemulsion phase, and excess oil.

phases (not given in Table I). The total recovered amount is smaller than the initial amount, which is probably caused by adsorption effects in combination with SDS in the column. Although hardly measurable, the lamellar phase seems to contain slightly more brine.

In the hexanol system, the lamellar and the microemulsion phases in the two-phase microemulsion/lamellar, the three-phase lamellar/microemulsion/oil, and the four-phase brine/lamellar/microemulsion/oil equilibria were analyzed. It appears that in the two-phase system the oil/brine ratio is approximately equal to 1 for both phases, but in the three- and four-phase systems, the lamellar phase contains almost twice as much brine as oil while the microemulsion phase contains slightly more oil. From gas chromatography measurements, it was found that the lamellar phase contains a little more hexanol than the microemulsion phase. From the results presented in Table I, it is clear that upon increasing the amount of surfactant in the system the SDS concentration in both the lamellar and microemulsion phases in the four-phase equilibrium increases. This phenomenon accounts for the observation that the volume of the surfactant-rich phases does not increase linearly with the surfactant concentration. This change in surfactant concentration in the lamellar and the microemulsion phase might be caused by the negative adsorption of salt at the large charged oil/brine interface, leading to an increasingly higher "effective" salt concentration as a function of the amount of SDS in the system, which in turn influences the interlamellar spacing. We will return to this issue in the Discussion section.

Small-Angle X-ray Scattering. In Figure 7, scattering curves of a typical microemulsion phase and a lamellar phase are shown. From a study of single-phase lamellar systems, it is found that the bump in the scattering curve corresponding to the lamellar phase reflects approximately the q value q_{max} at which a Bragg peak is expected. The peak position $D = 2\pi/q_{max}$ as a function of $1/x_s$ (with x_s the SDS concentration (w/w)) in the lamellar phase in single- and multiphase systems is given in Figure 8.

Solid lines are best-fit lines to the points corresponding to single lamellar phases. From the slopes of the best-fit lines, the molecular areas of SDS are deduced to be (0.73 ± 0.01) nm^2 in the pentanol system and (0.63 ± 0.01) nm^2 in the hexanol system, significantly lower than the molecular area obtained from interfacial tension measurements at the planar cyclohexane–brine interface being 0.93 nm^2 for both pentanol and hexanol systems.[22] The line corresponding to this value is also given in Figure 8. So from the

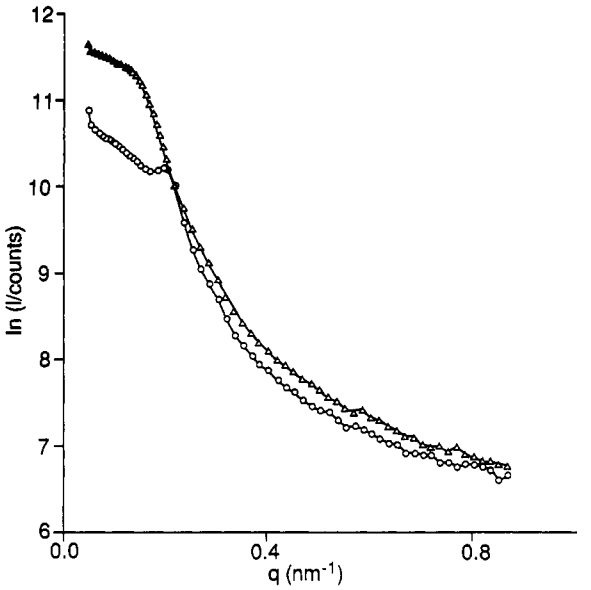

Figure 7. Scattering curves of a typical (coexisting) microemulsion phase (△) and a lamellar phase (○). x_h = 0.00. The lines are guides to the eye.

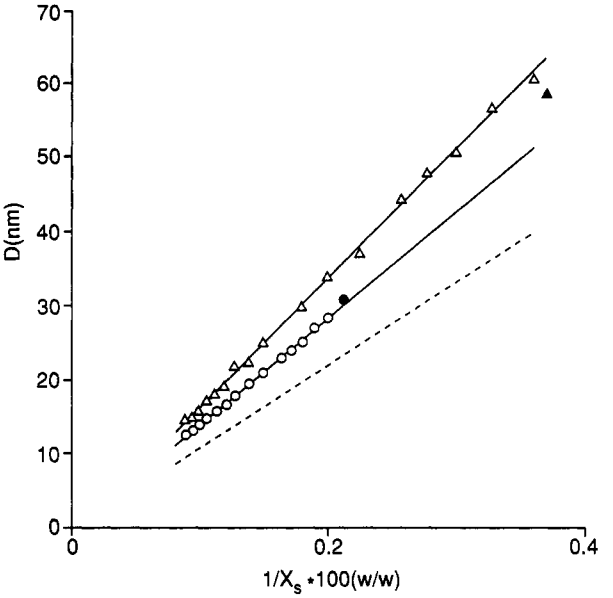

Figure 8. Bragg peak positions $2\pi/q_{max}$ versus $1/x_s$ with x_s the SDS weight fraction in the lamellar phase. Single-phase lamellar systems for $x_h = 0.00$ (○) and $x_h = 1.00$ (△) (empty symbols). Peak positions obtained from lamellar phases coexisting with a microemulsion phase are indicated by the corresponding filled symbols.

interlamellar spacing, an apparent total area smaller by a factor 0.78 (pentanol) and 0.68 (hexanol) is found. We will return to this point in the Discussion section.

In Table II, the values of D of the lamellar phases in the multiphase lamellar systems are given, to be compared to D_c calculated from the compositions given in Table I using

$$D_c = \frac{2M_s}{x_s N_A \rho_{L_\alpha} \sigma_{s,app}} \tag{10}$$

where M_s, x_s, N_A, ρ_{L_α}, and $\sigma_{s,app}$ are the molecular weight of SDS, the mass fraction of SDS (given in Table I), Avogadro's number, the density of the lamellar phase (being 0.90 g/cm^3 for systems with an oil/brine ratio of approximately 1 and 0.95 g/cm^3 otherwise) and the apparent molecular area of SDS obtained from SAXS, respectively.

Determination of Dispersion Sizes. The dispersion size ξ in the microemulsion phase defined by eq 1 is easily obtained from the

TABLE II: Comparison of Lamellar Spacings Obtained from Bragg Peak Positions in the Small-Angle X-ray Scattering Curves and D_c Calculated from the Compositions Given in Table I Using the Apparent Molecular Areas Deduced from Figure 8

total SDS concn (g/g)	coexisting phases	SAXS D (nm)	composition D_c (nm)
	Pentanol System		
0.0431	$L_\alpha/\mu E$	29	31
0.0472	$L_\alpha/\mu E$	29	31
	Hexanol System		
0.0028	$B/L_\alpha/\mu E/O$	110	104
0.0056	$B/L_\alpha/\mu E/O$	96	105
0.0083	$B/L_\alpha/\mu E/O$	89	86
0.0111	$B/L_\alpha/\mu E/O$ (top)[a]	72	72
	(middle)	81	–
	(down)	90	–
0.0167	$L_\alpha/\mu E/O$	61	63
0.0250	$L_\alpha/\mu E$	59	63

[a] Top, middle, and down refer to the height positions where the samples were taken.

TABLE III: Dispersion Size ξ in Middle-Phase Microemulsions as a Function of the Hexanol Mass Fraction x_h in the Cosurfactant Mixture Pentanol Plus Hexanol

x_h	ξ (nm)	x_h	ξ (nm)
0.00	35.8	0.75	68.5
0.25	44.4	1.00	72.0[a]
0.50	57.3		

[a] Lamellar phase present.

microemulsion volume $V_{\mu E}$ and the total area in the system $A = N_s\sigma_s$, with N_s and σ_s the number of SDS molecules and the area per molecule, by using

$$\xi = \frac{3V_{\mu E}}{2A} \tag{11}$$

where it is assumed that all the surfactant resides in the microemulsion phase. In the case of the system with pure hexanol as cosurfactant, a lamellar phase is present, and therefore we calculated ξ from the composition of the microemulsion phase by

$$\xi = \frac{6\phi_0\phi_w M_s}{N_A x_s \rho_{\mu E}\sigma_s} \tag{12}$$

in which $\rho_{\mu E}$ denotes the mass density of the microemulsion phase (0.90 g/cm^3). The dispersion sizes are presented in Table III, where we used $\sigma_s = 0.93$ nm^2 [22] and not $\sigma_{s,app}$, as the latter reflects properties of the lamellar phase and is not necessarily the real molecular area of SDS.

As shown in Table III, the dispersion size ξ in the microemulsion (middle) phase increases steeply as a function of the hexanol fraction in the cosurfactant mixture. This is directly related to the observation that the middle phase is swollen up to a one-phase microemulsion at the expence of the excess phases at increasingly lower surfactant concentrations.

Discussion

Phase Behavior and Length Scales. The almost linear behavior of the phase boundaries as presented in Figure 6 is qualitatively in agreement with the theoretical results depicted in Figure 2. A similar agreement was reported in ref 14, where theory and experiment on nonionic C_iE_j microemulsion systems (with i the chain length and j the head size) were compared. Therefore, we conclude that increasing the hexanol fraction x_h in the cosurfactant mixture in our ionic surfactant system has the same effect on the phase diagram as an increase of $i + j$ in a nonionic system, and both variations seem to increase K. One expects that a four-phase equilibrium water–lamellar–microemulsion–oil is reached as soon as the 3–1 and 1–2 phase boundaries intersect, as is indeed

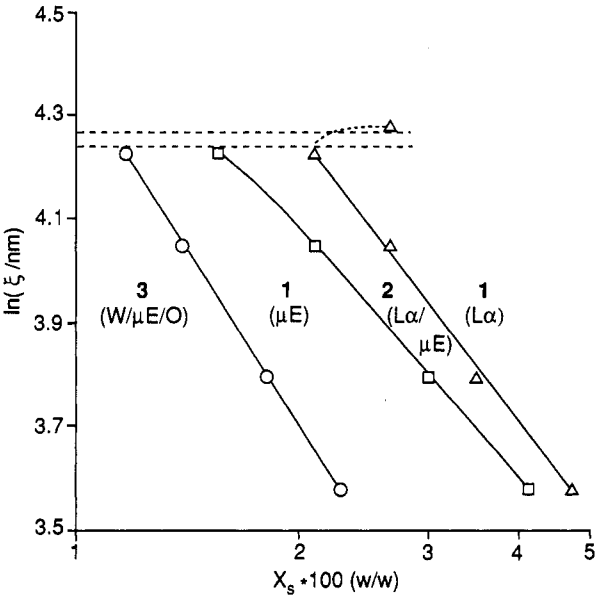

Figure 9. Phase boundaries in the $\ln(\xi)$–x_s plane. Symbols are the same as in Figure 6. Here again, the four-phase equilibrium appears between the boundaries indicated by dashed lines.

predicted theoretically.[5,6,14] Extrapolating the 3–1 and 1–2 phase boundaries (Figure 6) results in an intersection point higher than $x_h = 1.0$, where a lamellar phase in equilibrium with a microemulsion phase and two excess phases is observed experimentally. This suggests that the 3–1 and the 1–2 phase boundaries approach each other much more rapidly than is expected from the linear extrapolation of these lines. However, the relation between x_h and K is not *a priori* a linear one, but as mentioned in the theory section, in ref 15 experimental evidence is presented that $\ln \xi$ increases linearly with K. A more direct comparison with Figure 2 is therefore obtained by presenting the phase lines in the $(\ln \xi)$–x_s plane rather than in a x_h–x_s representation. This is shown in Figure 9.

If we leave out of consideration the point corresponding to $x_h = 1.00$, the phase boundaries in this double logarithmic representation again behave almost linearly. The 3–1 line is strictly linear as it is based on eq 11. However, the 1–2 line curves differently than predicted by theory. As mentioned above, the 3–1 line and the 1–2 line should intersect between $\xi \simeq 69$ and 72 nm (where the four-phase equilibrium appears), which can only be accomplished if the 1–2 line strongly curves toward the 3–1 line. Such a strong curvature of the 1–2 line toward the 3–1 line is not found in the theory of Andelman et al.[14] nor in the theory of Golubovic and Lubensky.[6] From inspection of Figure 3, where we plotted the 1–2 and the 2–1 lines in the $\bar{\kappa} - \log(\phi_s)$ plane, we observe that the 1–2 line has the appropriate curvature. This implies that an increasingly negative $\bar{K}$ as a function of the hexanol fraction in the cosurfactant mixture might be responsible for the experimentally observed curvature of the 1–2 line toward the 3–1 line. As pointed out in ref 12, it is indeed expected that $\bar{K}$ is negative for a surfactant monolayer and that it will decrease with the (co)surfactant chain length.[23,24] Therefore, our results indicate that (within the model under consideration) a simultaneously increasing K and a more negative $\bar{K}$ are responsible for the increasing stability of the lamellar phase compared to the microemulsion phase as a function of the hexanol fraction in the system studied here. In general, it is expected that both K and $\bar{K}$ will change with the fraction of cosurfactant (mixture) as well. However as shown by us recently,[22] the monolayer composition is the same for both pentanol and hexanol as cosurfactant, and it does not change above a cosurfactant weight fraction of 0.05 initial in oil. Therefore, we expect K and $\bar{K}$ to remain effectively constant for the weight fraction of cosurfactant (mixture) above this value.

From Table III and Figure 4, it follows that the increasing stability of the lamellar phase upon increasing x_h is accompanied by an increase of the dispersion size in the microemulsion phase. Above $\xi \simeq 70$ nm, the lamellar phase even becomes stable in the body of the fish. We wonder whether a similar limiting value can also be found in other surfactant systems. Lee et al.[25] reported the dispersion sizes in the nonionic systems C_8E_3 (in decane) and $C_{10}E_4$ (in octane) being 5.8 and 18.7 nm, respectively, much lower than the length scales observed in our system. In the $C_{10}E_4$ system, the lamellar phase is still relatively far away from the body of the fish, but it is much closer in the $C_{12}E_4$ system.[13] Now the lamellar phase almost touches the body of the fish. Assuming that the adsorption densities of $C_{10}E_4$ and $C_{12}E_4$ at the octane–water interface are equal, we can write

$$\xi_{C_{12}E_4} = \frac{c^*_{s,C_{10}E_4}}{c^*_{s,C_{12}E_4}} \xi_{C_{10}E_4} \tag{13}$$

where c^*_s is the molar surfactant concentration necessary to take up the excess water and oil phases (corrected for the critical micelle concentration). Using this relation, we estimate $\xi_{C_{12}E_4} \simeq 75$ nm, which is close to the value of $\xi = 72$ nm found for the hexanol system. Apparently, $\xi \simeq 70$–80 nm is an indication for the proximity of a lamellar phase to the middle-phase region in two different systems. *A priori*, one would expect that as soon as the lamellar phase is stable at a surfactant concentration at which the middle phase in the three-phase system is swollen up to a one-phase microemulsion, ξ and D will be of comparable size since $\xi \simeq 3V/2A$, $D = 2V/A$, and $V/A \propto 1/x_s$ in a system with equal volumes of water and oil, but there is no necessity for an "absolute" length scale or an upper limit for ξ. This limit may follow from model considerations comparing the free energies of the microemulsion phase and the lamellar phase. Here, an indication is found that such a limit exists by comparing two completely different systems.

Lamellar Phase in the Presence of Isotropic Phases. From the data presented in Table II, it follows that the agreement between D and D_c is satisfactory, which provides additional evidence that the birefringence phase in the three- and four-phase equilibria in the hexanol system has, indeed, a lamellar structure. Taking into account the volume fractions of oil and water given in Table I, it follows that in the two-phase coexistence region lamellar–microemulsion the oil and water interlamellar spacings $D_o = \phi_o D$ and $D_w = \phi_w D$ are approximately equal. However, as soon as more phases come into play (as is the case in the system containing pure hexanol), the situation becomes rather complicated. First of all, in the lamellar phase the oil–water symmetry is broken to the extent that $D_w \simeq 2D_o$, while at the same time in the microemulsion phase the oil/water ratio remains approximately equal to 1. Furthermore, in the four-phase region above a surfactant concentration $x_s = 0.006$ g/g, the interlamellar spacing decreases with increasing x_s. Whether or not this may be attributed to the effect of a negative adsorption of salt resulting in an increasing effective salt concentration and therefore a decreasing electrostatic repulsion between the lamellae as a function of the SDS concentration is still under study. Nevertheless, the combination of this observation with the larger interlamellar water spacing compared to the oil spacing leads us to the conclusion that, in spite of the rater high salt concentration we used, electrostatic effects still seem to play a role. Evans and Parsegian[26] directed attention to the possibility that thermal undulations may lead to a much slower decay of the electrostatic repulsion between charged bilayer membranes than expected from classical double-layer theory.[27] This effect was further elaborated by Pincus, Joanny, and Andelman;[28] Evans and Ipsen;[29] and Odijk.[30] The treatment by Evans and Ipsen[29] of the renormalization of the electric repulsion between membranes leads to the prediction that even for large separations there is still a considerable enhancement of the electrostatic repulsion. Whether this enhancement is sufficient to explain the experimentally observed asymmetry of the water and oil spacings requires detailed calculations, which we hope to address in a future publication.

A complicating factor is that in the four-phase system with $x_s = 0.011$ (somewhat lower than the surfactant concentration at which the water phase disappears) a gradient in interlamellar spacing seems to be present (Table I) and a slight increase of ϕ_w with increasing lamellar distance is observed (not shown). It is expected that the gradient in interlamellar spacing will be proportional to the gravity constant times the osmotic compressibility. The latter will increase upon increasing interlamellar spacing, and since the interlamellar spacing is quite high, the gradient apparently becomes considerable.

Variation of the Interlamellar Spacing with the SDS Concentration in Single-Phase Lamellar Systems. The smaller total area obtained from the interlamellar spacing compared to the one obtained using the Gibbs adsorption equation[22] is rather puzzling. Strey et al.[32] found a comparable discrepancy in a $C_{12}E_5$/octane/water system. As pointed out in ref 31, this difference may be attributed to a combination of strongly undulating monolayers and area-consuming defects. The influence of the first possibility will now be investigated. A logarithmic deviation from the linear (ideal) dilution law of the lamellar phase

$$D = \delta/\phi_s \tag{14}$$

with δ the thickness of the surfactant layer which can be written as $\delta = \bar{v}_s/\sigma_s$ where $\bar{v}_s$ is the surfactant molecular volume and ϕ_s the surfactant volume fraction was first described by Strey et al.[32] for a nonionic bilayer in water system. We will apply a similar analysis for the mixed monolayer system here.

In a fluctuating membrane system, thermal undulations tend to decrease the projected area, while the total area A is conserved. A first-order correction to the projected area A_{proj} of a membrane caused by thermal undulations is[33]

$$\frac{A}{A_{proj}} = 1 + \frac{k_B T}{4\pi K} \ln\left(\frac{q_{max}}{q_{min}}\right) \tag{15}$$

where q_{max} and q_{min} are the upper and lower wavenumber cutoffs

$$q_{max} = 2\pi/a; \quad q_{min} = 2\pi/\lambda \tag{16}$$

with a again a molecular length scale and λ the deflection length

$$\lambda = c'u(K/k_B T)^{1/2} \tag{17}$$

where c' is a model-dependent constant of order unity[33,34] and u is the root mean square of the amplitude of the undulations. In a lamellar phase with only short-range steric repulsions between the membranes, the deflection length is directly proportional to the interlamellar distance D as in that situation $u \propto D/2$ (recall that D is defined here as the sum of the water and oil spacing). Using eq 14–17 then leads to a dilution law of the form[32,36]

$$D\phi_s/2 = A - B \ln(\phi_s) \tag{18}$$

in which

$$A = \delta\left(1 + \frac{k_B T}{4\pi K} \ln\left(\frac{c''\delta}{a}(K/k_B T)^{1/2}\right)\right) \tag{19}$$

and

$$B = \delta k_B T/4\pi K \tag{20}$$

with c'' a constant of order unity.

In parts a and b of Figure 10, we plot $D\phi_s/2$ against $\ln(\phi_s)$. According to eq 18, the slope of the line is a measure of the "hidden" area caused by thermal undulations of the monolayers. If undulation repulsion would indeed dominate in our system, which is to be expected for a salt concentration of 0.2 M (in that case the Debye length is approximately 0.7 nm, being of the same order of magnitude as in ref 35 where no indications for electrostatic repulsions are found), we would expect $B \simeq 0.05$–

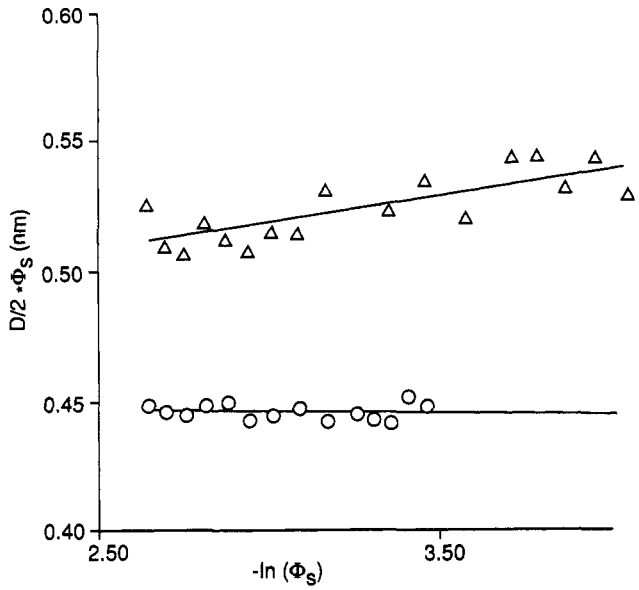

Figure 10. Data from Figure 8 plotted as $(D/2)\phi_s$ versus $-\ln(\phi_s)$. Straight lines correspond to a best fit of the data to eq 18.

1.2 nm (δ varied between 0.5 and 1.5 nm and K between 0.1 and 1 k_BT). However, we found values for B that are much lower: close to zero for the pentanol system and $B = (0.020 \pm 0.004)$ nm for the hexanol system. This implies that undulation repulsion does *not* dominate and that electrostatic repulsion plays an important role. In that case, the deflection length is given by eq 17 but now u depends in a complicated way on D. In principle, the value of u can be determined from self-consistent mean field theories of charged multimembrane systems.[29,30] However, the situation is complicated by the fact that in a system containing an extensive charged surface a substantial amount of co-ions will be negative adsorbed, leading to a larger effective salt concentration. We calculated the effective salt concentration from the co-ion adsorption using the Poisson–Boltzmann equation. We found a steep increase as a function of the SDS concentration ranging from 0.25 M at $x_s = 0.055$ to 0.33 M at $x_s = 0.11$. At constant interlamellar spacing, it is expected that an increasing salt concentration will increase u (the amplitude of the undulations will increase since the Debye length decreases). Therefore, although the interlamellar spacing decreases as a function of the SDS concentration (which tends to decrease u), this may be more or less compensated by the concomitant change in the effective salt concentration having the opposite effect on u. This effectively results in a lower $\ln \phi_s$ dependence of the interlamellar spacing compared to what may be expected for systems without electrostatic interactions. In this light, we would like to note that Roux et al.[36] performing the same analysis (i.e., eqs 18–20) on several bilayer systems, found indications that at a salt concentration of 0.2 M undulation repulsion dominates. For the pseudoternary monolayer systems studied here, however, indirect evidence is presented that even at salt concentrations higher than 0.2 M electrostatic interactions are still present. A possible explanation for this difference is that in our system K might be lower, leading to more pronounced electrostatic repulsion enhancement.

The larger slope in Figure 8 implies that the hexanol system "hides" more surface than the pentanol system, presumably caused by the relatively large interlamellar spacing. Indeed, fitting the data in Figure 8 for the hexanol system up to $x_s = 0.067$ (w/w) reveals a molecular area of (0.71 ± 0.03) nm^2, approximately equal to the one obtained for the pentanol system. This, however, does not explain the discrepancy with the area obtained with another method.[22] As our analysis of the thermal undulations is obscured by some complicating electric double-layer effects, it is at this stage not possible to distinguish the separate contributions from thermal undulations and defects.

Concluding Remarks

From this work, some interesting conclusions can be drawn. First of all, it is shown that the competition between the lamellar and the microemulsion phase at vanishing spontaneous curvature can be tuned by the variation of the hexanol fraction in a cosurfactant mixture consisting of pentanol and hexanol. Upon increasing the hexanol fraction in the cosurfactant mixture, the lamellar phase becomes stable at increasingly lower surfactant concentration. At the same time, the dispersion size in the microemulsion (middle) phase increases. Above a certain value of the dispersion size (approximately 70 nm), the lamellar phase becomes stable in the body of the fish, leading to a different and rather complicated pattern of phase behavior. This value of the dispersion size is comparable to the one estimated for a nonionic system,[13] where the lamellar phase is close to the body of the fish. A speculative explanation for this observation may be that this is the length scale at which the entropy of mixing oil and water domains becomes too small to compensate for the curvature free energy of the microemusion phase.

The comparison of our experimental results with a phenomenological theory[5] reveals that the competition between the lamellar and the microemulsion phase is qualitatively correctly described by theory. A more quantitative comparison points to the necessity to include K.

From the study of the lamellar phase in the systems with pure pentanol and with pure hexanol as cosurfactant, several indications are found for the presence of fluctuation-enhanced electrostatic repulsion. These indications are as follows: (a) the larger interlamellar water spacing compared to the oil spacing ($D_w \simeq 2D_o$) in the lamellar phase coexisting with a microemulsion phase and one or more excess phases, (b) the decreasing interlamellar distance in the lamellar phase upon increasing x_s in the four-phase (hexanol) systems above $x_s \simeq 0.006$ (g/g), and (c) the much lower slope of $D\phi_s/2$ versus $\ln \phi_s$ in the single-phase lamellar systems (Figure 10) compared to what may be expected.[36]

As far as point (a) is concerned, it was pointed out to us by an anonymous referee that also in nonionic surfactant systems the lamellar phase appears to be more stable on the aqueous than on the oleic side. Therefore, the observation described under point (a) by itself does not necessarily indicate the existence of enhanced electrostatic repulsion.

Acknowledgment. The authors thank M. H. Tollenaar for drawing the figures, Bonny Kuipers for his help with the SAXS equipment, Theo Odijk for enlightening discussions, and an anonymous referee for pointing out to us the last remark in the Conclusion section. The investigation was supported by the Netherlands Foundation of Chemical Research (SON) with financial aid from the Netherlands Organization for Scientific Research (NWO).

References and Notes

(1) Kahlweit, M.; Strey, R.; Busse, G. *J. Phys. Chem.* **1990**, *94*, 3881.
(2) Bellocq, A. M.; Biais, J.; Bothorel, P.; Clin, B.; Fourche, G.; Lalanne, P.; Lemaire, B.; Lemanceau, B.; Roux, D. *Adv. Colloid Interface Sci.* **1984**, *20*, 167.
(3) Talmon, Y.; Prager, S. *J. Chem. Phys.* **1978**, *69*, 2984.
(4) Jouffroy, J.; Levinson, P.; de Gennes, P. G. *J. Phys. (France)* **1982**, *43*, 1241.
(5) Andelman, D.; Cates, M. E.; Roux, D.; Safran, S. A. *J. Chem. Phys.* **1987**, *87*, 7229.
(6) Golubovic, L.; Lubensky, T. C. *Phys. Rev. A* **1990**, *41*, 4343.
(7) Widom, B. *Langmuir* **1987**, *3*, 12.
(8) Gompper, G.; Schick, M. *Phys. Rev. B* **1990**, *41*, 9148.
(9) Strey, R. *Habilitationsschrift*; Göttingen, 1992.
(10) van Aken, G. A. Thesis, Rijksuniversiteit Utrecht, 1990.
(11) Hackett, J. L.; Miller, C. A. *SPE Reservoir Eng.* **1988**, *3*, 791.
(12) Kegel, W. K.; Lekkerkerker, H. N. W. Accepted for publication in *Colloids Surf.*
(13) Kahlweit, M.; Strey, R.; Firman, P. *J. Phys. Chem.* **1986**, *90*, 671.

(14) Cates, M. E.; Andelman, D.; Safran, S. A.; Roux, D. *Langmuir* **1988**, *4*, 802.
(15) Langevin, D. *Adv. Colloid Interface Sci.* **1991**, *34*, 583.
(16) Helfrich, W. *J. Phys.* (*France*) **1985**, *46*, 1263.
(17) Peliti, L.; Leibler, S. *Phys. Rev. Lett.* **1985**, *54*, 1960.
(18) Helfrich, W. *Z. Naturforsch.* **1978**, *33a*, 305.
(19) Roux, D.; Coulon, C.; Cates, M. E. *J. Phys. Chem.* **1992**, *96*, 4147.
(20) Hartshorne, N. H.; Stuart, A. *Crystals and the Polarizing Microscope*; Edward Arnold: London, 1970.
(21) Strey, R., personal communication.
(22) Kegel, W. K.; Aken, G. A.; van Bouts, M. N.; Lekkerkerker, H. N. W.; Overbeek, J. Th. G.; de Bruyn, P. L. *Langmuir* **1993**, *9*, 252.
(23) Helfrich, W. in Les Houches, Session XXXV, 1980. *Physics of Defects*; Balian, R., et al., Eds.; North Holland: Amsterdam, 1981; p 715.
(24) Szleifer, I.; Kramer, D.; Ben-Shaul, A.; Gelbart, W. M.; Safran, S. A. *J. Chem. Phys.* **1990**, *92*, 6800.
(25) Lee, L. T.; Langevin, D.; Meunier, J.; Wong, W.; Cabane, B. *Progr. Colloid Polym. Sci.* **1990**, *81*, 209.
(26) Evans, E. A.; Parsegian, V. A. *Proc. Natl. Acad. Sci. U.S.A.* **1986**, *83*, 7132.
(27) Verwey, E. J. W.; Overbeek, J. Th. G. *Theory of Stability of Lyophobic Colloids*; Elsevier: Amsterdam.
(28) Pincus, F.; Joanny, J. F.; Andelman, D. *Europhys. Lett.* **1990**, *11*, 763.
(29) Evans, E.; Ipsen, J. *Electrochim. Acta* **1991**, *36*, 1735.
(30) Odijk, T. *Langmuir* **1992**, *8*, 1690.
(31) Strey, R.; Winkler, J.; Magid, L. *J. Phys. Chem.* **1991**, *95*, 7502.
(32) Strey, R.; Schomäcker, R.; Roux, D.; Nallet, F.; Olsson, U. *J. Chem. Soc., Faraday Trans.* **1990**, *86*, 2253.
(33) Helfrich, W.; Servuss, R. M. *Nuovo Cimento* **1984**, *3D*, 137.
(34) Golubovic, L.; Lubenski, T. C. *Phys. Rev. B* **1989**, *39*, 12110.
(35) Nallet, F.; Roux, D.; Prost, J. *Phys. Rev. Lett.* **1989**, *62*, 276. Roux, D.; Safinya, C. R. *J. Phys.* (*France*) **1988**, *49*, 307.
(36) Roux, D.; Nallet, F.; Freyssingeas, E.; Porte, G.; Bassereau, P.; Skouri, M.; Marignan, J. *Europhys. Lett.* **1992**, *17*, 575.